journal homepage: www.brodogradnja.fsb.hr

Brodogradnja

An International Journal of Naval Architecture and Ocean Engineering for Research and Development

Corrosion-induced thickness diminution of an ageing bulk carrier

Nataša Kovač[1], *Špiro Ivošević*[2*], *Nikola Momčilović*[3]

[1] *University of Donja Gorica, Faculty of Applied Sciences, Oktoih 1, Donja Gorica, Podgorica, Montenegro*
[2] *University of Montenegro, Faculty of Maritime Studies Kotor, Put I Bokeljske brigade 44, Kotor, Montenegro*
[3] *University of Belgrade, Faculty of Mechanical Engineering, Kraljice Marije 16, Beograd, Serbia*

ARTICLE INFO

Keywords:
Ship corrosion
Inner bottom plates
Corrosion depth
Deterministic and stochastic model

ABSTRACT

The 2030 Agenda for Sustainable Development introduced 17 Sustainable Development Goals (SDGs). The International Maritime Organization (IMO) has endorsed connections between the maritime sector and SDGs, emphasising sustainable production in the marine environment. Consequently, technical considerations, such as ship structure sustainability, are crucial for marine safety. The impact of corrosion influences the structural degradation of vessels and the risk of structural failure and fuel oil spills significantly. The formulation of predictive corrosion models, grounded in historical data accumulated during vessel operations, emerges as an optimal strategy for designing structural elements and guaranteeing their structural integrity. This paper analyses non-linear deterministic and stochastic corrosion models, focusing on an ageing bulk carrier, to provide design-phase information for sustainable structures. Utilising data on measured steel plate thickness over a 20-year operational period, non-linear models are employed to calculate the millimetres of thickness diminution. Assuming corrosion onset at 7, 8, and 9 years, corresponding coefficients are computed, based on the developed model. A model is also considered, in which there were no assumptions about the beginning of corrosion initiation. The corresponding annual corrosion rate was observed separately in each of the models, as a deterministic variable and as a probabilistic random variable. This approach aims to enhance the understanding of the causal relationship between corrosion processes and structural performance, contributing to the development of sustainable design practices in the maritime industry.

1. Introduction

Recognising the challenges facing humanity today, the United Nations adopted the Sustainable Development Agenda until 2030 in 2015 [1]. The Agenda includes 17 specific goals (Sustainable Development Goals – SDG) related to the plan of action for people, the planet and prosperity. Recognising

* Corresponding author.
E-mail address: spiroi@ucg.ac.me

http://dx.doi.org/10.21278/brod75404
Received 12 March 2024; Received in revised form 2 August 2024; Accepted 8 August 2024
Available online 20 August 2024
ISSN 0007-215X; eISSN 1845-5859

the importance that sustainable development has for the entire community, IMO considered and approved the linkages between the IMO's technical assistance work and the 2030 Agenda for Sustainable Development [2].

Although each of the goals has significance for the social community, the IMO has recognised that the greatest significance in terms of the marine industry has highlighted SDGs (4-7, 9, 13, 14 and 17), and denoted those most directly relevant to IMO's technical assistance work [2], see Figure 1. Among these goals, considering the topic of this paper, three are particularly significant: SDG 7: Ensure access to affordable, reliable, sustainable, and modern energy for all, SDG 13: Take urgent action to combat climate change and its impacts, and SDG 14: Conserve and use the oceans, seas, and marine resources sustainably for sustainable development.

Fig. 1 IMO and the sustainable development goals diagram [3]

In recent decades, significant efforts have been made to optimise ship design and implement Regulations to enhance safety and sustainability. Numerous Regulations were passed in previous years to reduce environmental pollution caused by the emission of exhaust gases from ships, and to apply new renewable energy sources, all to use the oceans, seas, and marine resources sustainably for sustainable development. To address climate change, emissions and more sustainable design, the IMO introduced short- and long-term goals while delivering energy efficiency Regulations for new and existing ships, refer to [4-7]. This is expected to propel their technological development and reduce pollution significantly. Further studies on energy efficiency policy for ships can be found in [8], while the impact of climate change on ship design is elaborated in [9].

Given that the majority of material goods are transported by ships, new challenges are imposed on vessels to focus on sustainable maritime transport through optimal design and the selection of suitable renewable energy sources. In this sense, with proper design and optimal use of resources, it is possible to have sustainable and clean ships, and meet the set goals of sustainable development.

As the ships are designed for 25 years, interventions on the design are quite demanding, and, among other things, require considerable research in terms of design optimisation, vessel weight, energy consumption during the life cycle and reduction of exhaust gas emissions. For example, optimising and reducing the ship's lightweight mass through appropriate maintenance and predicting element thickness reduction (e.g., due to corrosion) is linked directly to the ship's energy efficiency, as its weight impacts power demand significantly. Moreover, with proper design and maintenance, ships can be kept in operation for a longer period, and their inevitable recycling can be directed to the designed one, or postponed for a longer period. Often, due to

collisions, damage, and the age of construction, their lifespan is shortened, and they are scrapped earlier. To make maximum use of the projected life cycle of the ship, it is necessary to analyse the possibility of exploitation of the ship during the designed life cycle based on historical data. In this sense, this paper analyses the impact of corrosion in an old bulk carrier that has been in operation for 20 years. Analysing the damage during exploitation a non-linear model is developed, so that the corrosion margin can be predicted on its basis and the ship's design can be intervened before its construction. In such a way, extensive work in steel would be reduced, potential pollution would be prevented, and the harmful impact of ships would be reduced on society in general.

This paper is structured in 6 sections. The second section provides a comprehensive review of ship corrosion, while the third section presents the relevant database and non-linear corrosion models. The results are presented in the fourth section. Following this, the fifth section engages in a discussion of the main findings. Finally, the sixth section offers concluding considerations.

2. Ship corrosion

Numerous research studies have identified bulk carriers and tankers as types of ships associated with a high number of incidents. Recent research has confirmed that general and dry cargo vessels exhibit the highest likelihood of casualties [10-12]. Furthermore, different analyses of maritime incidents or evaluations of operational risks for general cargo ship operators can assist in optimising vessel performance [13].

Numerous maritime incidents over the past decades attracted special attention from researchers, who tried to detect degrading factors and take measures to prevent unwanted consequences and prolong the life cycle of vessels. Different types of defects can occur on the surface of specific structure areas of a ship’s hull. Coating breakdown, cracks, deformation, corrosion, fouling or fatigue, can decrease the safety of the vessel and projected life significantly. Due to different environments, operation life, maintenance procedures, ship`s route etc., different corrosion forms can be found. General corrosion, pitting, intergranular, galvanic, stress-corrosion, corrosion fatigue, fretting, microbiological, crevice, erosion and cavitation can be found in different ship hull areas and at different times of exploitation of a vessel [14].

There are different directions in the degrees of the corrosion process. In some research, the authors develop different corrosion models, or investigate the chemical or mechanical properties of materials and their behaviour under conditions of different environments [15-17]. Also, simulations have proven to be an indispensable tool for the design and optimisation of naval vessels, such as in the research of cavitation flows, especially around the propeller and rudder [18].

A new protective coating can be used to optimise vessel life and reduce the negative degradation effects such as corrosion[19]. Performance Standards were implemented for protective coating -PSPC in April 2006, and they can be expected to improve the coating quality efficiency. Especially, different preventative biofouling monitoring techniques can be used to provide sustainable shipping, achieve better energy efficiency of the vessel, and reduce the biofouling of a ship’s hull [20]. Furthermore, corrosion can be decreased by scarifying anodes, but the impressed current cathodic protection (ICCP) scheme is a more reliable and efficient method of a corrosion prevention mechanism [21]. In that sense, the weight of different corrosion protective types and their influence on hull protection and the design purpose of the hull should be considered [22].

Numerous studies in similar domains have focused on researching individual or entire structural areas or hull elements, such as plates and stiffeners. Research conducted by the Class NK Classification Society focused on the number of incidents in different structural areas of ageing vessels, and proved that ballast tanks and cargo holds are most susceptible to various types of damage caused by corrosion, while cargo holds and other vessel areas are slightly less susceptible to corrosion [23].

Cargo holds experience significant decay due to corrosion, and the examination of the structural elements and areas that are susceptible to intensive corrosive processes is, therefore, of the utmost importance. Particularly critical areas are shell plates in the cargo hold (on single-skin bulk carriers) and the mainframes. One side of the shell plates is in direct contact with the external environment, while the internal side is in contact with cargo from the cargo holds. Double-hulled ships were built over the last decades to increase

security. Previous research focused on the inner bottom plating [17, 24], cargo hold transverse bulkheads [25], cargo hold mainframes [26], or the main deck [27].

Research on the inner bottom plating, as a part of the cover of double bottom tanks, is highly important, because the inner bottoms contain cargo in the holds and represent a zone that is exposed to complex environmental conditions. Maintenance and cargo operations, along with manipulative equipment, have a dominant influence on the corrosion process of the upper part of the inner bottom plating.

From the underside of plates, intensive ballast operations, wet-dry cycles and partially filled tanks, often create the conditions for accelerated development of corrosion, as shown in Figure 2.

Fig. 2 Inner bottom plating: a) the bottom side of water ballast tanks, b) corroded peace of the inner bottom as a part of a fuel oil tank

The basis for the development of corrosion models includes the understanding of the length of exposure to environmental influences, and measured data on the thickness diminution of certain structural elements. The largest possible database should indicate the amount of measured data, vessel characteristics, etc. Corresponding models should show corrosion rate and depth, describe the corrosion process, predict the corrosion margin, etc.

Many authors confirmed that the corrosion process is unstable and time-dependent. The rate of corrosion can be described by linear or non-linear models. Generally, the corrosion process has two dominant phases. In the first phase, there is no actual corrosion and the protective coating is still effective. In the second phase, after the degradation of the coating, the corrosion process starts at the time of exposure. Some authors describe the corrosion process in the second phase as an aerobic and anaerobic process [28].

There are numerous corrosion models which assume that the corrosion rate has a constant value. For instance, Guedas Soares and Garbatov [29] developed a non-linear model, Yamamoto et al. [30], Paik et al. [31-34] developed a three-phase model, while Melchers developed a four-phase [35, 36] and five-phase model [37].

Previous studies by the same authors examined mainly linear models of corrosion, which were very efficient for the description of the corrosion processes on certain structural areas of corresponding ships [17, 24, 38, 39]. It was based on the resulting linear model of the corrosion depth (d) obtained from $d = c_1(t - T_{cl})^{c_2}$ when coefficient $c_2 = 1$. T_{cl} is the time when the corrosive processes begin, the coefficient c_1 represents the corrosion rate, while coefficient c_2 shows a functional dependence of the corrosion depth on the time influence. However, this article analyses the non-linear dependence of corrosion depth based on time and defines different values of c_2.

3. Materials and methods

In this context, structural integrity refers to the actual material degradation of the particular elements due to corrosion-induced diminution, evaluated for the inner bottom plating of bulk carriers.

This paper is based on the analysis of historical data on the thickness diminution of the structural areas of inner bottom plating that is a part of the cover of fuel oil tanks on ageing bulk carriers in operation. The systematisation of measured data and the analysis of a non-linear corrosion model were performed, based on the thickness-measuring data that were collected during regular special surveys (after 10, 15 and 20 years). The thickness diminution of the inner bottom plating was expressed in millimetres of wear following the collected and systematised data. The research relies on a non-linear corrosion model in which the values of c_1 and c_2 coefficients were determined concerning the available data, assuming that corrosion begins 7, 8 and 9 years after building the ship. Note that the authors do not investigate the source of the corrosion (general, pitting, etc.) which precedes the thickness diminution of the elements. We seek to evaluate the latter - an actual consequence in that context.

In our previous research [24, 38, 39], which included a larger base of ships that transported coal, iron ore and other more corrosive cargoes, it was observed that the corrosion process started earlier, based on coating breakdown and thickness measurements of corrosion reduction. In the subject research, less corrosive cargo and transhipment operations that did not require heavy manipulative equipment did not cause the beginning of corrosion during the first 5 years of exploitation. The lack of data between two special surveys, i.e., between 5 and 10 years of exploitation, motivated us to vary the start of corrosion from 7 to 9 years. Also, our research has shown that the corrosion process starts later with the particular ship, and, for that reason, we varied the value from 7 to 9 years.

3.1 The database on corrosion damage

The ship was built by Class NK mild steel grade A with a minimum yield strength of 235 MPa. Figure 2.b shows the corroded part of the replaced inner bottom plate, as a part of our previous work, in which the chemical composition shows different corrosion processes from the cargo hold and fuel oil tanks [40]. Namely, corroded pieces of the inner bottom plating, which was faced to the cargo hold, detected only iron (Mean 62.53%), oxygen (Mean 34.95%) and a small amount of chloride ions (2.52%). On the surface that faced the fuel tank, in addition to iron (Mean 9.41%), oxygen (Mean 47.05%) and chloride ions (Mean 1.56%), the analysis detected inorganic ions such as manganese (Mean 1.13%), sodium (Mean 1.23%), aluminium (Mean 2.86%) and silicon (Mean 11.89%), and the organic components carbon (Mean 22.75%) and sulphur (Mean 0.48%) [40].

The measurements on vessels were performed following the rules of classification societies which define the scope of measurement clearly. Each structural area was accordingly subjected to adequate measurements that observed the condition of the structures over time.

The measurements were performed by an authorised company (see Acknowledgment) for thickness measurement of the ship's hull structure, and operators who performed the measurements following the classification rules. The scope and locations of measurement were performed in line with specific types of the classification survey. The standard acoustic-based testing equipment, which comprised a transmitter that emits ultrasonic waves and a receiver that receives the reflected waves, was used to measure the thickness of the inner bottom plating without surface painting. The detailed procedure of measurement, systematisation and processing of data in accordance with the created methodology of obtaining appropriate data is presented in earlier works of the author [24, 38, 39].

The inner bottom plating of bulk carriers covers fuel oil tanks, ballast tanks and dry space. According to our extensive research, in previous work the inner bottom plating above the fuel oil tanks was investigated, as plates with intensive corrosion, compared to the other inner bottom plating which covers the water ballast tanks and dry space. Furthermore, the deepest corrosion was located in contact areas close to the side water ballast tanks, where dynamic changes of water and dry cycles were exchanged due to ballast operations.

The paper analyses an old bulk carrier during a 20-year exploitation cycle. The measurements conducted on each fuel tank were systematised, and the obtained data are shown in Table 1. Four fuel oil tanks were analysed, along with 210 measuring points. Only general corrosion wastage was considered. The systematisation of measures means that each tank was divided into 5 sections, and that one value was taken from each cross-section sheet [24, 38, 39].

Table 1 The scope of measuring the average corrosive damage

Years	**10 years**	**15 years**	**20 years**
Damage in mm	0.5	1.4	1.8
Number of measurements	70	70	70

The analysis was performed for a total of 210 corrosion depth measurements, that were obtained through three special surveys of an ageing bulk carrier. Figure 3 shows 210 inputs for further analysis. More precisely, 70 measurements were observed after 10, 15, and 20 years of the ship's operation. These data can be used to inform predictive maintenance models, where corrosion depth measurements can help predict future corrosion and plan maintenance before critical levels are reached. An equal number of measurements at each survey point ensures that comparisons across periods are statistically robust, providing a reliable empirical database for analysing ship corrosion behaviour over time.

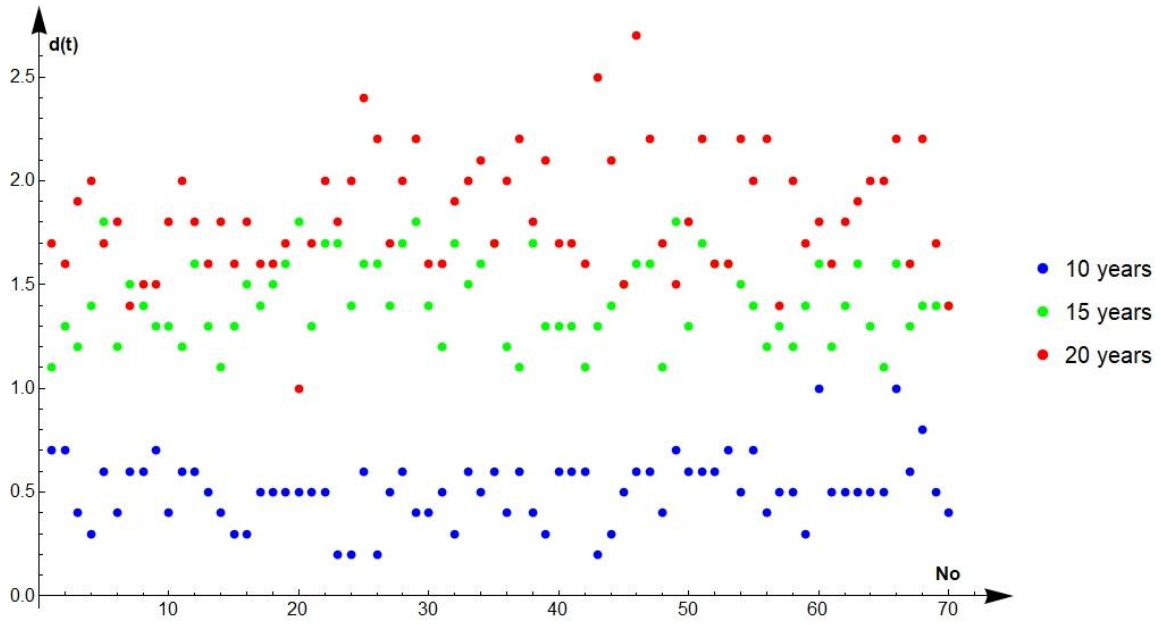

Fig. 3 The empirical database of corrosion depth measurements, corrosion depth *d(t)* [mm], length of the operation of a ship *t* [years]

Three groups of measured data are shown in different colours in Figure 3. The ordinal number of measurements is shown on the x-axis, while the measured value of corrosion depth is shown on the y-axis.

The values of the basic descriptive statistics were calculated for each of the three data groups. The results are shown in Figure 4 as box and whisker [41]. The minimum and maximum values of corrosion depth, the first and third quartiles, as well as the median, are shown for each data group. The values are shown on the right side of the box and whisker graphs, while the median is additionally illustrated by a black line. The left side of the graph presents the mean values, which are, additionally, shown by a white line on the graph.

These types of plots are useful for understanding the distribution and central tendency of corrosion data at different time intervals, and can be critical for planning maintenance and predicting the lifespan of ships or other structures exposed to environmental factors.

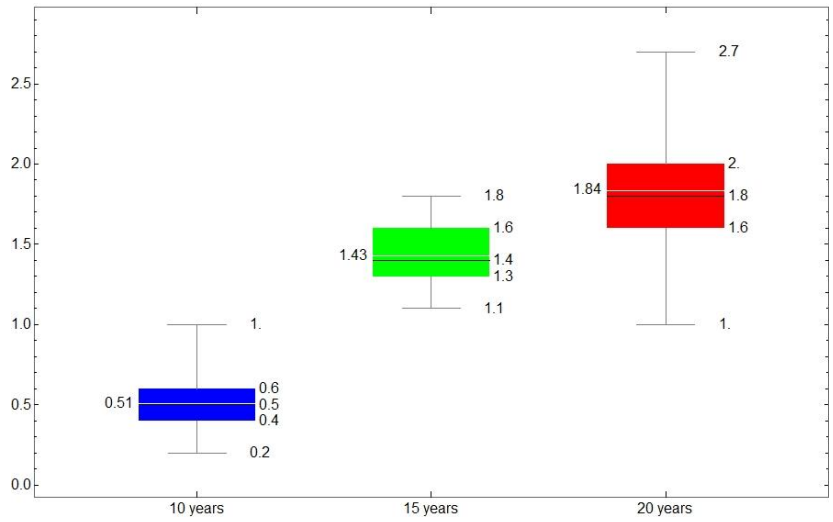

Fig. 4 The descriptive statistics of the observed groups of empirical data on corrosion depth

The corrosion data for 10 years is less spread out, with the median value around 0.51. The interquartile range (the length of the box) is very narrow, indicating less variability in the data. There are no outliers, and the range (the difference between maximum and minimum) is quite small. In the case of the green plot (i.e., 15 years), the median value has increased to around 1.43, suggesting an increase in the central tendency of corrosion. The interquartile range is wider than at 10 years, indicating more variability in the data. There are no visible outliers, and the range has increased, showing that the extreme values of corrosion have also increased. For 20 years (red box), the median value has increased further, to approximately 1.84, showing a trend that corrosion is worsening over time. The interquartile range remains relatively similar to the 15-year data, suggesting a consistent variability over the last 5 years. There are no potential outliers indicated. However, the maximal observed value is significantly higher than the rest of the data, with a value of around 2.7. This could represent an extreme case of corrosion.

There is a clear upward trend in the median value of corrosion as the time increased from 10 to 20 years, indicating that corrosion generally worsens over time. The variability of the corrosion measurements also increased with time, as can be seen from the widening of the interquartile range. The presence of a potential outlier at 20 years could indicate an extreme case, or a different corrosion mechanism that is not present in the other data.

The gradual increase in the median and range of the data over time suggests that the corrosion rate accelerates as the ship ages. This can be due to several factors, such as material degradation, changes in environmental exposure, or less effective maintenance as the vessel ages. The increasing trend in corrosion depth and variability implies that, as a ship ages, the risk of unpredictable and potentially severe corrosion increases, which can have significant implications for maintenance schedules, safety and operational costs.

3.2 Non-linear corrosion model

One of the most common models describing the depth of corrosion of structural elements on ships is found in the studies by Paik [32] and Qin & Cui [42]. The basis of a non-linear model is the understanding of the onset of corrosive processes. In non-linear modelling, the depth of corrosion is considered a dependent quantity, whose value is expressed in years, and obtained as a degree function of the length of ship operation. The functional dependence of the corrosion depth $d(t)$ can be represented in the following way:

$$d(t) = c_1(t - T_{cl})^{c_2}, t > T_{cl} \tag{1}$$

In equation (1), t denotes the length of the operation of a ship, while T_{cl} represents the time when corrosive processes began. In other words, T_{cl} represents the length of protective action of anti-corrosion coatings. The coefficients c_1 and c_2 are real and positive unknown parameters of the model. If the c_2 parameter of the model equals 1 ($c_2 = 1$), the model then represents a linear dependence of corrosion depth on time (t).

For other values of the c_2 parameter, the model considers $d(t)$ a non-linear variable. The coefficient c_1 represents the corrosion rate and is usually expressed in mm/year. The functional dependence of the depth of corrosion on the influence of the time component is regulated by the c_2 coefficient. According to Paik et al. [25], the c_2 variable can have the values of 1 or 1/3. Previous studies [24, 38, 39], analysed a linear corrosion model with the proposed value $c_2 = 1$. In this paper, statistical analysis aims to determine the values of all three unknown parameters of the model (c_2, c_1, T_{cl}). In that way, the model would describe the empirical database of corrosion depth of the Inner Bottom Parts (IBP) structure adequately. Therefore, this analysis is not limited to the proposed values of the c_2 parameter and the corresponding c_1 parameter. The analysis determines the most favourable values experimentally, depending on the selected value of T_{cl}. Since the c_2 parameter does not have a limiting value of 1, this study examines the depth of corrosion as a non-linear dependent variable. Statistical analysis was performed with a significance level of 0.05, i.e., 95%, and confidence intervals were calculated for the model parameters. The Akaike information criterion (AIC) [43] was used as the criterion for the selection of the best-fitting model.

4. The results of the corrosive diminution of the inner bottom parts

The application of the corrosion model represented by equation (1) assumes that corrosive processes start after 7, 8, and 9 years. Following this hypothesis, the values of 7, 8, and 9 were included in equation (1), thus forming the corresponding models of the corrosion depth of the IBP structure which are denoted by $d_7(t), d_8(t), d_9(t)$, respectively. The most favourable values of the c_1 and c_2 parameters were determined by employing the statistical techniques of fitting models to empirical data, for each corrosion model formed. Additionally, the model represented by equation (1) was fitted to the empirical data on the corrosion depth of the IBP structure without any limitations and assumptions. The model can, thus, be observed concerning the three unknown parameters. This model, labelled with $d_b(t)$, resulted in a model that describes the empirical data best. Table 2 shows the results of the fitting of the proposed models to the empirical data on the corrosion depth of the IBP structure.

Table 2 The table of parameters for the fitting of the corrosion models

Parameters		**Estimate**	**S-Error**	**Confidence interval [mm]**	**t-statistic**	**p-value**
$T_{cl} = 7$ [years]	c_1 [mm]	0.26	0.02	(0.22, 0.29)	13.4464	$4.49\text{x}10^{-30}$
	c_2	0.75	0.03	(0.72, 0.84)	24.7719	$5.71\text{x}10^{-64}$
$T_{cl} = 8$ [years]	c_1 [mm]	0.37	0.22	(0.32, 0.41)	16.9446	$4.87\text{x}10^{-41}$
	c_2	0.66	0.03	(0.61, 0.71)	25.1392	$5.73\text{x}10^{-65}$
$T_{cl} = 9$ [years]	c_1 [mm]	0.55	0.02	(0.50, 0.59)	23.0214	$4.12\text{x}10^{-59}$
	c_2	0.51	0.02	(0.47, 0.55)	25.308	$2.00\text{x}10^{-65}$
$T_{cl} = 9.64$ [years]	c_1 [mm]	0.75	0.07	(0.61, 0.90)	10.2238	$4.01\text{x}10^{-20}$
	c_2	0.38	0.04	(0.30, 0.47)	8.87517	$3.34\text{x}10^{-16}$

The inclusion of the values of c_1 and c_2 parameters from Table 2 into the corrosion models $d_7(t), d_8(t), d_9(t), d_b(t)$ provided adequate models for the depth of corrosion, as shown by equations (2) - (5):

$$d_7(t) = 0.26(t-7)^{0.75}, t > 7 \tag{2}$$

$$d_8(t) = 0.37(t-8)^{0.66}, t > 8 \tag{3}$$

$$d_9(t) = 0.55(t-9)^{0.51}, t > 9 \tag{4}$$

$$d_b(t) = 0.75(t-9.64)^{0.38}, t > 9.64 \tag{5}$$

Figure 5 presents the models obtained graphically. The curvature of the curves illustrates the reduced rate of corrosive processes over time, which is the consequence of the formation of a corrosive layer on the surface of the IBP structures.

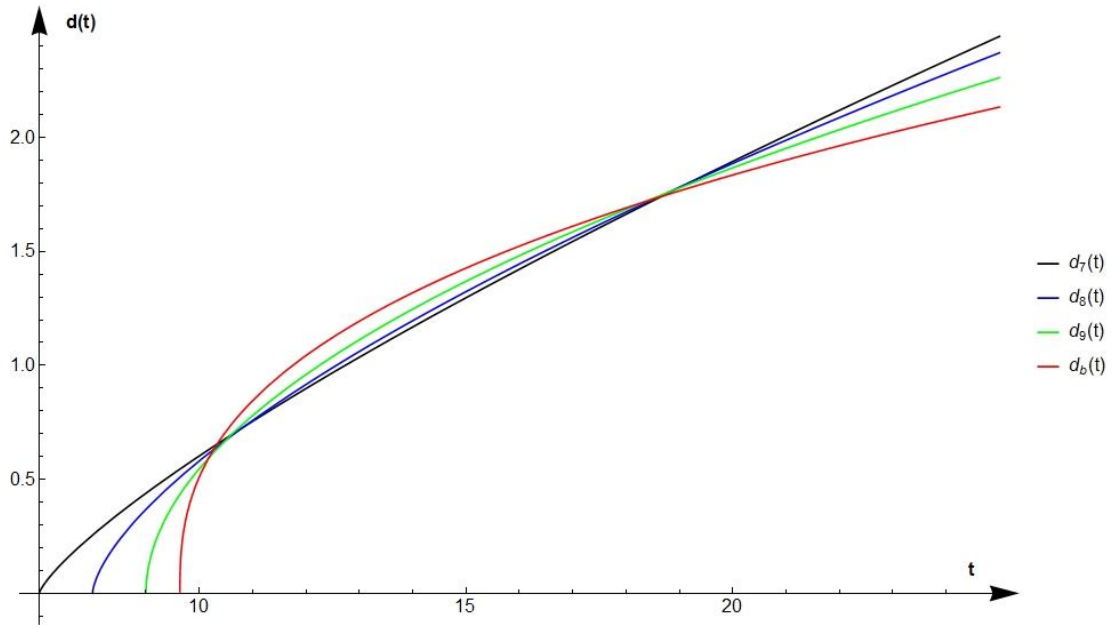

Fig. 5 A graphic representation of the formed corrosive models

The Analysis of Variance (ANOVA) was performed to collect information about the levels of variability within a fitted model, and to conduct the tests of significance [44]. The ANOVA Tables were defined for all models, represented by equations (2) through (5). Tables 3-6 show the results of the ANOVA analysis for the fitted models represented by equations (2) through (5), as well as the degree of freedom (Df), the sum of squares (SS), and mean squares (MS).

Table 3 The ANOVA table for model (2) with $T_{cl} = 7$

$d_7(t)$	Df	SS	MS
Model	2	394.63	197.32
Error	208	12.38	0.06
Uncorrected Total	210	407.01	
Corrected Total	209	74.87	

Table 4 The ANOVA table for model (3) with $T_{cl} = 8$

$d_8(t)$	Df	SS	MS
Model	2	395.39	197.69
Error	208	11.62	0.06
Uncorrected Total	210	407.01	
Corrected Total	209	74.87	

Table 5 The ANOVA table for model (4) with $T_{cl} = 9$

$d_9(t)$	Df	SS	MS
Model	2	396.27	198.13
Error	208	10.75	0.052
Uncorrected Total	210	407.01	
Corrected Total	209	74.87	

Table 6. The ANOVA table for model (5) with $T_{cl} = 9.64$

$d_b(t)$	Df	SS	MS
Model	3	396.67	132.22
Error	207	10.34	0.05
Uncorrected Total	210	407.01	
Corrected Total	209	74.87	

The minimum SS value of 10.34 was calculated for the $d_b(t)$ model. The calculation of the value of the F-ratio and the corresponding p-value of a fit can be performed concerning the results shown in Tables 3-6. The F-ratio in an ANOVA Table is calculated as the Mean Square of the Model (MS Model) divided by the Mean Square of the Error (MS Error). It is used to determine whether the model explains significantly more variance in the data than what would be expected by chance. The corresponding p-value then helps to assess the statistical significance of this result.

The calculated F-ratios for models (2) through (5) are 3315.57, 3537.37, 3835.85, and 2646.47, respectively. All the F-ratios values are very high, which suggests that the models are significantly better at explaining the variation in the data than would be expected by chance. The p-value of all models is below 0.000, which indicates a good performance of the fitted models concerning the measures from the empirical database.

The AIC criterion of model selection was also performed, bearing in mind that it is particularly useful when comparing different models fitted to the same dataset. For the proposed models (2) through (5), the AIC can be determined as:

$$AIC = n \cdot ln(RSS/n) + 2k \tag{6}$$

where k is the number of parameters in the model, n is the sample size, and RSS is the residual sum of squares. A model with a lower AIC is generally considered better, because it captures a balance between complexity (number of parameters) and goodness of fit.

For models (2)-(5), the AIC was calculated based on formula (6), resulting in values -588.54, -601.74, -618.28, -624.29, respectively. The model denoted as $d_b(t)$ had the lowest AIC value, which confirms the assumption that the model represented by equation (5) is the most adequate for the prediction of future corrosion depth values. The ANOVA results for this model show a very low SS value, indicating minimal deviation from the empirical data, and the lowest AIC value, confirming it as the most adequate predictive model.

The corrosion models $d_7(t)$, $d_8(t)$, $d_9(t)$, and $d_b(t)$ reflect the corrosive diminution of the IBP of a ship starting at different times, with the T_{cl} values indicating the clear times of 7, 8, and 9 years respectively. These models are differentiated by their parameter values c_1 and c_2, which were optimised to fit the empirical corrosion data.

The early start of corrosion is captured by the $d_7(t)$ and $d_8(t)$ models. These models assume that corrosion starts relatively early in the ship's life. The $d_7(t)$ model has a lower c_1 value but a higher c_2, indicating a steep initial increase in corrosion depth that decelerated over time. The $d_8(t)$ model has a higher c_1 value, indicating that, once corrosion starts (after 8 years), it does so with a greater initial depth. However, the exponent c_2 is lower than in $d_7(t)$, suggesting a slower increase in corrosion depth over time.

Later start of corrosion is represented by the $d_9(t)$ model, which assumes a later start to corrosion and has the highest c_1 value, suggesting a substantial initial corrosion depth once it begins. The c_2 value is the lowest among the three, indicating that, after the initial depth, the rate of increase in corrosion is the slowest.

The $d_b(t)$ model suggests that corrosion starts at $T_{cl} = 9.64$ years, a time derived from fitting the model to the data without preset assumptions. It has the highest c_1 value, indicating a significant initial corrosion depth, but the lowest c_2 exponent, suggesting the gentlest increase in corrosion depth over time.

In models (2)-(5), parameter c_1 is considered as a deterministic variable. Moving on to the stochastic observation of the c_1 parameter, the inherent uncertainty and variability present in real-world scenarios are

included in the consideration. This decision to treat c_1 as a random variable was driven by the availability of empirical data and the need to balance model complexity with computational feasibility. This kind of model strikes a balance between accuracy and practicality, providing meaningful insights while remaining computationally manageable.

In corrosion studies, deterministic models, while providing valuable insights through fixed interdependencies of the model variables, often fail to capture the complex and unpredictable nature of environment-material interactions. Stochastic modelling introduces a probabilistic dimension to the parameter c_1, allowing it to vary according to a particular distribution. This approach, on the one hand, increases the realism of the model, and, on the other hand, provides a more detailed understanding of the potential range and probability of different corrosion outcomes, which is essential for comprehensive risk assessment and decision-making in marine vessel management.

To ensure that the parameter c_1 is treated as a stochastic variable, it is possible to transform model (1) in the following way:

$$c_1(t) = \frac{d(t)}{(t-T_{cl})^{c_2}}, t > T_{cl} \tag{7}$$

Variations of the model (7) for different values of T_{cl}, will be explored, to incorporate the temporal aspect of corrosion occurrence effectively in the stochastic modelling approach. This entails adapting the parameter c_2 to align with the specific T_{cl} values. Consequently, the models for c_2 tailored to these specific instances will be referred to as $c_1^{model\,(n)}$, where n represents the values in the set $\{7, 8, 9, b\}$. This notation connects each stochastic model of c_2 directly to its corresponding deterministic model, as outlined in models (2) through (5). This approach allows drawing parallels, and making direct comparisons between the deterministic and stochastic models, enriching the understanding of how temporal factors influence corrosion processes.

Table 7 shows statistics that provide a comprehensive picture of the distribution of the formed datasets for parameter c_1 depending on different values of parameters T_{cl} and c_2. The mean value (column Mean) and Standard Deviation (column Std. Deviation) describe the centre and spread, respectively, while asymmetry (column Skewness) and column Excess Kurtosis provide information about the shape of the distribution, especially about its symmetry and the presence of outliers.

Table 7 Descriptive statistics for c_1 parameters in different models

Model	Mean	Std. Deviation	Skewness	Excess Kurtosis
$c_1^{model\,(7)}$	0.26	0.06152	-0.32	0.78
$c_1^{model\,(8)}$	0.36	0.07947	-0.16	1.46
$c_1^{model\,(9)}$	0.54	0.11671	0.04	2.30
$c_1^{model\,(b)}$	0.75	0.16351	0.45	3.38

Analysing and comparing the descriptive statistics of the parameter c_1 across models $c_1^{model\,(7)}$ to $c_1^{model\,(b)}$ reveals both similarities and differences in their distributions.

Model $c_1^{model\,(7)}$ has a lower mean (0.26) compared to other models, as well as a relatively small Standard Deviation (0.06152) indicating less variability. It is characterised by negative skewness (-0.32) which suggests a slight leftward skew, while excess kurtosis (0.78) indicates a slightly heavier tail than a normal distribution. Model $c_1^{model\,(8)}$ has less skew (-0.16) compared to model $c_1^{model\,(7)}$, suggesting a more symmetric distribution. Its higher excess kurtosis (1.46) indicates more pronounced tails. The same holds for the model $c_1^{model\,(9)}$ with near-zero skewness (0.04), and substantially higher excess kurtosis (2.30). The largest Standard Deviation (0.16351) is observed in model $c_1^{model\,(b)}$ indicating the most variability among

the models. This model has positive skewness (0.45), and very high excess kurtosis (3.38), indicating very pronounced tails.

The mean, as well as the Standard Deviation in the models, increases as the value of the T_{cl} parameter increases, suggesting that the variability of c_1 increases with each model. The skewness changes from negative in the model $c_1^{model\,(7)}$ to positive in the model $c_1^{model\,(b)}$, indicating a shift in the distribution's symmetry. The excess kurtosis increases across models, suggesting that the distributions become more leptokurtic (having more pronounced tails) in the higher models.

In the following, a statistical analysis of the c_1 parameter was performed, characterising it as a stochastic variable. In this sense, standard probabilistic distributions were fitted to the calculated values of each data set ($c_1^{model\,(7)}$ to $c_1^{model\,(b)}$), to discover the one that describes changes in the value of the parameter c_1 best. The distributions were not limited by the number of parameters, i.e., in the analysis, were considered two-parameter, three-parameter and multi-parameter distributions.

The characteristics of probability distributions are defined through the parameters of shape, location and scale. Each type of parameter has its specific purpose. The shape parameters determine the shape of the fitted distribution. Distributions with multiple shape parameters are more flexible than distributions with one shape parameter, in the sense that they can model a wider range of data behaviours. Each shape parameter controls different aspects of the shape of the distribution, allowing finer adaptation of the model to the complex behaviours of the processes being modelled. The location parameter translates the distribution along the x-axis. It has similar characteristics to the mean values in a normal distribution, but it does not always have to represent the central tendency. The scale parameter stretches or compresses the distribution along the horizontal axis, or, in other words, affects the spread or dispersion of the distribution. However, with complex distributions, this parameter also acquires complex characteristics, and does not always have to correspond to the Standard Deviation.

One of the key steps in statistical analysis, which involves fitting theoretical distributions with empirical data, is measuring the goodness of fit. These methods offer insight into the model's effectiveness in capturing the underlying patterns and characteristics of the data. The goodness of fit involves assessing how well the chosen distribution model represents the observed data, and can be performed using various statistical tests. A commonly used test is the Kolmogorov-Smirnov (KS) test, which compares the empirical distribution function with the theoretical cumulative distribution function.

In the process of statistical modelling of the stochastic characteristics of parameter c_1, many standard theoretical distributions were considered. Based on the KS test, the following distributions proved to be the best fit for the observed models $c_1^{model\,(7)}$ to $c_1^{model\,(b)}$:

- Three-parameter Log-logistic distribution for $c_1^{model\,(7)}$,
- Four-parameter Burr distribution for $c_1^{model\,(8)}$,
- Three-parameter Log-logistic distribution for $c_1^{model\,(9)}$,
- Two-parameter Gamma distribution for $c_1^{model\,(b)}$.

The values of belonging parameters of these best-fitted distributions are shown in Table 8.

Table 8 Values of the best-fitted distributions in different models describing c_1 parameters

Model	Distribution	Shape param.	Location param.	Scale param.
$c_1^{model\,(7)}$	Log-logistic	106055296.69	-3572375.84	3572376.11
$c_1^{model\,(8)}$	Burr	34.43 0.65	-0.89	1.27
$c_1^{model\,(9)}$	Log-logistic	33066675.16	-2051030.17	2051030.71
$c_1^{model\,(b)}$	Gamma	19.97	0	0.04

Please note that, in the case of Gamma distribution, when the location parameter is fixed at zero, the Gamma distribution is described only by its shape and scale parameters, making it a two-parameter distribution.

The probability density function (PDF) and the cumulative distribution function (CDF) are used to describe different aspects of the probability distribution of a random variable [45].

A PDF is used to determine the probability of a random variable falling within a specified range of values. For continuous distributions, the PDF is a function that describes the probability (density) of the random variable taking on a particular value. The area under the PDF curve within a given interval represents the probability that the random variable falls within that interval. Consequently, it is concluded that the total area under the PDF curve for all possible values is always 1. The PDF can help in understanding the shape of the distribution, especially where its values are most likely to occur.

The CDF can be obtained by integrating the PDF, and is a function that measures the probability that a random variable will be less than, or equal to, a certain value. The CDF starts at 0 and increases monotonically to 1. It can be used to describe the probability that a random variable will fall below, or above, a certain threshold.

Figures 6 and 7 show the corresponding PDF and CDF of the best-fitted distributions, whose parameters are given in Table 8. Along with each distribution graph, there are also histograms of the empirical data obtained based on formula (7) in which the value of T_{cl} is varied.

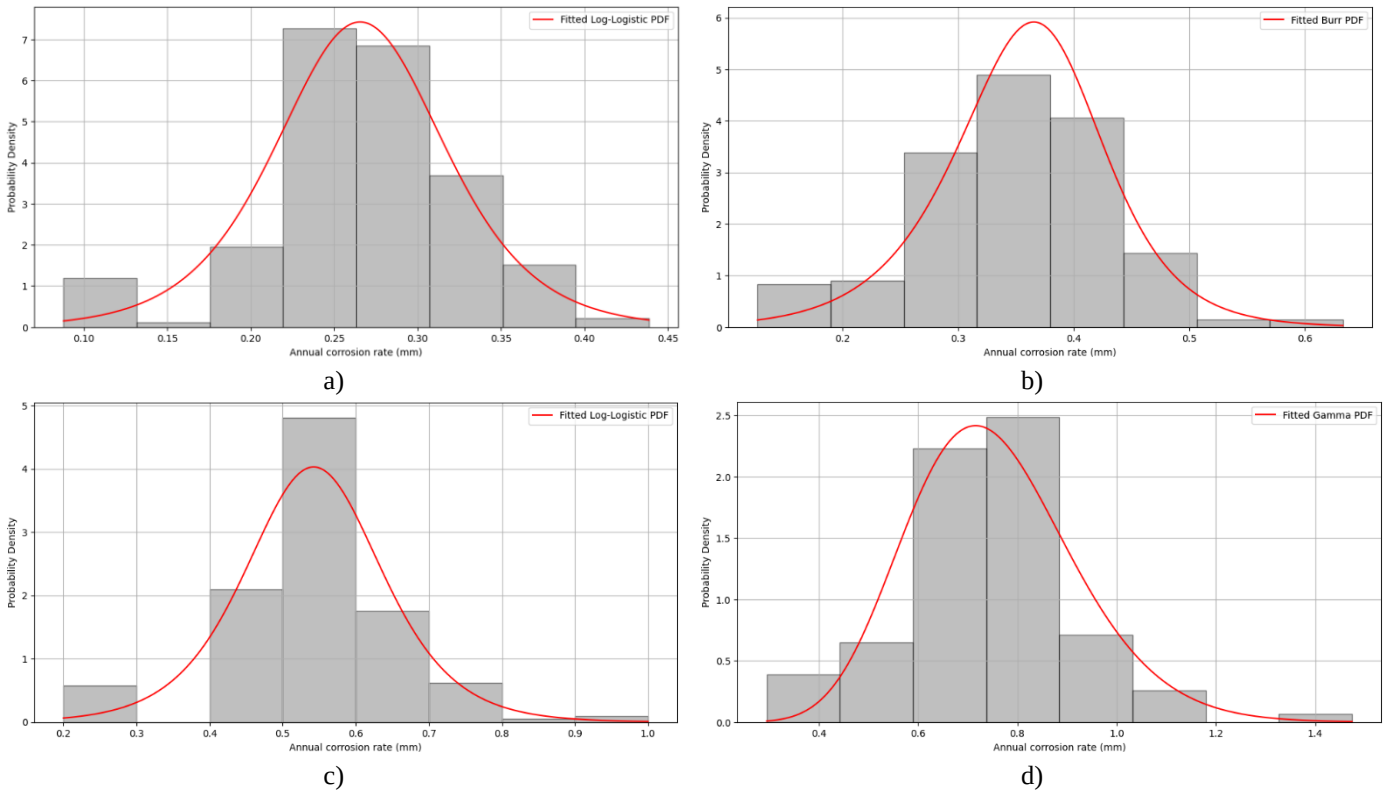

Fig. 6 Histograms of empirical c_1 Values and PDFs of best-fitted distributions: a) Log-logistic distribution for $c_1^{model\ (7)}$, b) Burr distribution for $c_1^{model\ (8)}$, c) Log-logistic distribution for $c_1^{model\ (9)}$, d) Gamma distribution for $c_1^{model\ (b)}$.

For mutual comparison of such complex probability distributions and their PDF or CDF, it is possible to use the methodology described in one of the works of the author of this manuscript [46].

The Kolmogorov-Smirnov goodness of fit test (KS test) was applied, to determine whether the empirical data and the fitted theoretical functions had the same distribution [47]. The null hypothesis assumes that the data come from the specified distribution, while the alternate hypothesis states that at least one value does not match the specified distribution. The results of the KS test are shown in Table 9.

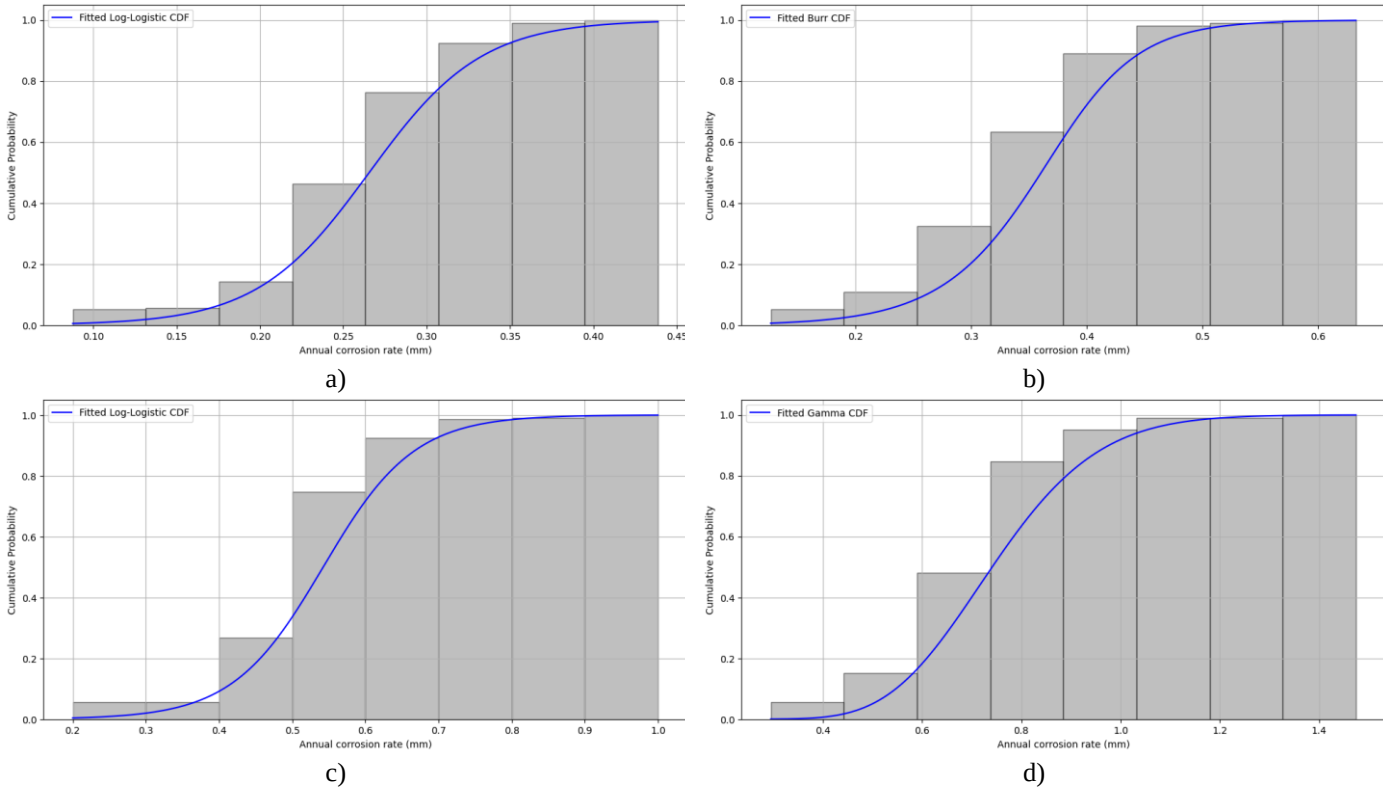

Fig. 7 Cumulative histograms of empirical c_1 Values and CDFs of the best-fitted distributions: a) Log-logistic distribution for $c_1^{model\,(7)}$, b) Burr distribution for $c_1^{model\,(8)}$, c) Log-logistic distribution for $c_1^{model\,(9)}$, d) Gamma distribution for $c_1^{model\,(b)}$.

The KS test was applied at a significance level of 98%, which corresponds to a critical value of 0.10475. The values of the KS statistic and the corresponding p-value were calculated for each observed model. The model is considered to describe the empirical data better if the value of the test statistic (Column 3 in Table 9) is lower, while the value of the p-value (Column 4 in Table 9) should be higher. If the statistic value is less than the critical value, the null hypothesis is accepted with a confidence level of 98%. Based on the KS goodness of fit test and under the assumption that the confidence level is 98%, the best-performing stochastic model is $c_1^{model\,(7)}$.

Table 9 Kolmogorov-Smirnov goodness of fit statistics

Model	Distribution	Statistics	p-value
$c_1^{model\,(7)}$	Log-logistic	0.07742	0.15308
$c_1^{model\,(8)}$	Burr	0.08062	0.12349
$c_1^{model\,(9)}$	Log-logistic	0.07876	0.14006
$c_1^{model\,(b)}$	Gamma	0.10272	0.02209

Figure 8 shows the models' outputs for $d(t) = c_1(t - T_{cl})^{c_2}, t > T_{cl}$ when T_{cl} takes values from set $\{7, 8, 9, 9.64\}$ and, consequently, parameter c_2 takes values from set $\{0.75, 0.66, 0.51, 0.38\}$. At the same time, the parameter c_1 follows the previously described Log-Logistic, Burr, Log-Logistic, and Gamma distributions, resulting in four different models for corrosion depth, denoted as $d_7(t)$, $d_8(t)$, $d_9(t)$, and $d_b(t)$. More precisely, parameter c_1 behaves as model $c_1^{model\,(7)}$, $c_1^{model\,(8)}$, $c_1^{model\,(9)}$, and $c_1^{model\,(b)}$, respectively.

The blue lines represent individual realisations of the model with different samples of c_1 from its distribution, while the red line shows the mean model using the average value of c_1. As t increases, the spread of potential model outputs increases due to the variability of c_1. The yellow shaded area represents this confidence interval, within which there is a 95% confidence that the true value of the model output will fall,

given the variability in c_1. The confidence interval widens as t increases, reflecting the increasing uncertainty in the model output over time. This visualisation can help in understanding the uncertainty in the model predictions over time.

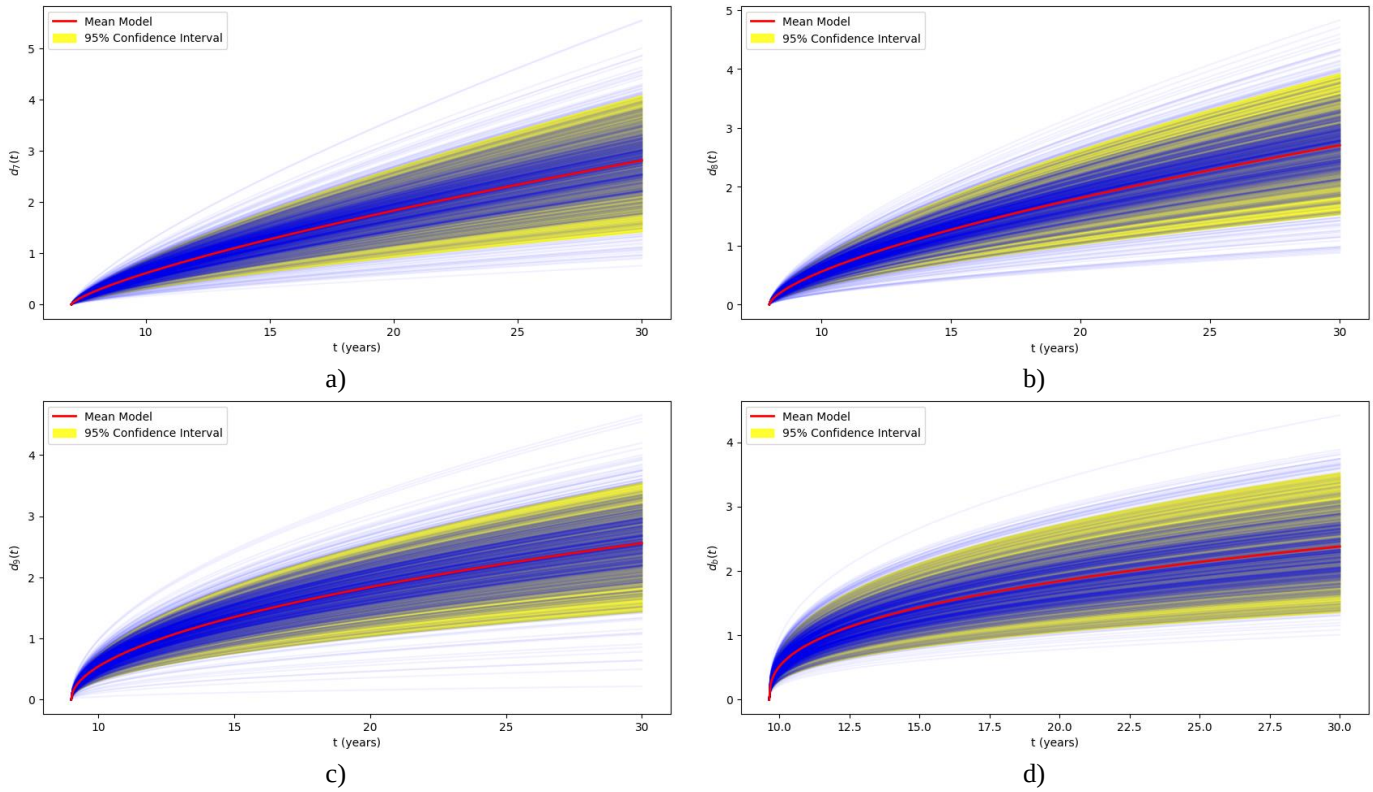

Fig. 8 Stochastic models of corrosion depth d(t)[mm] with a 95% confidence interval when parameter c_1 follows the best-fitted distributions: a) Log-logistic distribution for $c_1^{model\ (7)}$, b) Burr distribution for $c_1^{model\ (8)}$, c) Log-logistic distribution for $c_1^{model\ (9)}$, d) Gamma distribution for $c_1^{model\ (b)}$.

This plot not only illustrates the central tendency of the model, but also provides a visual representation of the variability and uncertainty inherent in the model's predictions. In Figure 8, each model is simulated over 1,000 different samples of c_1 values. By plotting many samples, it is possible to get a sense of the variability and range of outcomes that the model predicts. The red line indicates the average or expected value of the model across samples, i.e., it represents the central tendency of the model predictions. This mean model serves as a benchmark or reference point for understanding the typical behaviour expected of the distribution, given the input parameters.

The red curves from Figure 8 have the following analytical forms:

$$d_7(t) = 0.2655(t-7)^{0.75}, t > 7 \tag{8}$$

$$d_8(t) = 0.3578(t-8)^{0.66}, t > 8 \tag{9}$$

$$d_9(t) = 0.5424(t-9)^{0.51}, t > 9 \tag{10}$$

$$d_b(t) = 0.7537(t-9.64)^{0.38}, t > 9.64 \tag{11}$$

Notice that the deterministic values of the parameter c_1 in models (2)-(5) are very close to the mean values of the parameter c_1 obtained in models (8)-(11) when c_1 is modelled as a random variable following the considered probabilistic distribution.

5. Discussion

Until now, many authors have proposed different linear and non-linear corrosion models. Some corrosion models were developed for different structural areas (ballast tanks, main deck, etc.), or different structural elements (Paik et al. developed a model for 23 structural elements). The beginning of corrosion is related to the cracking of the surface paint, which was assumed based on historical data, or was monitored during the exploitation of the ship to determine the exact beginning of the corrosion process.

In this paper, the corresponding coefficients in the corrosion model were chosen based on the assumptions of the beginning of corrosion after 7, 8, and 9 years. Respecting this assumption, the corresponding annual corrosion rate was considered separately for a deterministic variable and as a probabilistic random variable.

The proposed models in this work show differences in statistical properties, which implies that each model represents different characteristics of the corrosion process. The increasing mean and variability suggest that later models may capture more severe or accelerated corrosion scenarios. These models can be used to predict future corrosion, which could lead to more efficient and cost-effective maintenance strategies.

The difference in the best corrosion initiation time values for deterministic ($T_{cl} = 9.64$) and stochastic models ($T_{cl} = 7$) reflects the characteristic nature of corrosion development and the way these two types of models handle variability and uncertainty. While deterministic models provide a general overview based on typical conditions, stochastic models incorporate the randomness and variability characteristic of real-world corrosion processes. The detected corrosion initiation difference can be attributed to several factors:

Deterministic models use fixed parameters and simplified assumptions to represent typical conditions, while stochastic models incorporate randomness and variability, capturing the irregularities and uncertainties inherent in corrosion processes better.

A deterministic model generally produces a single, fixed outcome based on given input parameters. The value of $T_{cl} = 9.64$ years in the deterministic model suggests that, under average or expected conditions, this is the estimated time for significant initiation of corrosion.

Stochastic models consider variability and uncertainty in input parameters. The best T_{cl} value of 7 years in the stochastic model may reflect a more realistic scenario, where variability in environmental conditions, material properties or other factors is considered.

The difference in T_{cl} values between the models indicate that, when real-world uncertainties and variability are considered, corrosion may start somewhat earlier than the more idealised deterministic model predicted.

A stochastic model, which considers variability, could capture more realistic scenarios where corrosion-accelerating factors (such as aggressive environmental conditions, fluctuations in protective measures or material inconsistencies) are present. Corrosion progression is not linear, and can be accelerated or slowed down by many factors. The stochastic approach provides a framework for modelling this irregular progression more accurately than deterministic models, which might overlook sudden changes or fluctuations.

The key difference between the deterministic and probabilistic approaches lies in the treatment of the parameters. The deterministic approach uses fixed parameter values with associated confidence intervals (Table 2 and red line in Figure 8), while the probabilistic approach models the variability of at least one parameter as a random variable, leading to a more comprehensive representation of uncertainty. While the deterministic approach provides confidence intervals for the parameters, it treats them as fixed values within these intervals (Formulas (2)-(5)). In contrast, the probabilistic approach explicitly models the variability of c_1 as a random variable. Both approaches involve fitting curves to empirical data. However, the probabilistic approach extends this by considering the distribution of the parameter c_1, leading to a range of potential outcomes rather than a single deterministic curve. The probabilistic model generates multiple realizations of the corrosion depth over time, each corresponding to a different sample from the probability distribution of c_1. This results in a spread of possible corrosion depths, which can be visualized as a confidence band or a set of curves representing different scenarios (Figure 8).

Our current probabilistic approach represents a balance between the available data, computational feasibility, and the need to capture the primary source of variability in the corrosion process. In our study, we treated c_1 as a random variable to account for the primary source of variability in the corrosion process. This decision was based on the significant influence of c_1 on the model outcomes and the available empirical data supporting this approach. While c_2 and T_{cl} were treated as fixed parameters, their values were determined through rigorous statistical fitting to the empirical data. This allowed us to focus on the dominant source of uncertainty, represented by c_1.

A fully probabilistic approach would involve treating all parameters c_1, c_2, and T_{cl} as random variables. One of the primary reasons for focusing on c_1 as the random variable is the limitation of available data. Comprehensive probabilistic modeling of all parameters requires extensive data to estimate the probability distributions of c_2 and T_{cl} accurately. Treating multiple parameters as random variables increases the computational complexity of the model. While this approach provides a more detailed uncertainty analysis, it also requires more sophisticated statistical techniques and computational resources.

Comparing the Common Structural Rules for Bulk Carriers and Oil Tankers, we can conclude that corrosion addition in the way of inner bottom plating is 3.7 mm from cargo holds and 0.7 from fuel oil tanks. In total, 4.4 mm. Considering our research, the estimated time when corrosion starts and average corrosion rate of 0.75mm/year, it can be concluded that the corrosion process exceeds the recommended rules, which motivates us to investigate corrosion in the contact areas of fuel tanks further.

6. Conclusions

To address the level of thickness diminution of elements and the sustainability of the ship structure, the paper analyses the corrosion effect for the inner bottom plating of the fuel oil tank on an ageing bulk carrier. The analysis depended vastly on the operating time which was considered an independent variable. The study observed a non-linear model that was previously found in the relevant literature, and whose three parameters are labelled as $c_2, c_1,$ and T_{cl}. In this paper, statistical analysis was carried out in two directions, deterministic and stochastic modelling of corrosive processes.

Detailed statistical analysis of deterministic and stochastic models presents a comprehensive view of the corrosion process. Statistical analysis provides a deeper understanding of the corrosion process affecting the ship, which is essential for planning long-term maintenance and ensuring the ship's structural integrity. It offers a customised approach for maintenance, based on the ship's age and the specific corrosion model that fits its empirical data best. Therefore, the main result of this paper is a series of specific, easy-to-use, non-linear corrosion model formulations, designed for predicting the corrosion-induced thickness diminution of inner bottom plating in bulk carriers. This is particularly crucial, considering that the inner bottom plating is among the most degraded parts of bulk carriers due to frequent loading and unloading sequences.

Regarding the deterministic corrosive model, the existing literature proposed the values of 1 or 1/3 for the c_2 parameter, depending on the degree of temporal influences on corrosive processes. The statistical analysis showed that the prescribed values of the c_2 parameter cannot provide the best-fitting models for the IBP structure. Namely, the best-developed model that can predict the future values of the corrosion depth of an IBP structure has the c_2 parameter that equals $c_2 = 0.38$ and the assumed onset of corrosion after 9.64 years. The average annual corrosion rate c_1 is estimated at 0.75 mm/year.

Allowing for stochastic variability in the values of parameter c_1, the modelling showed that the beginning of corrosion initiation occurs somewhat earlier than the deterministic model shows. Namely, if the uncertainties (the influence of the environment, material characteristics, maintenance, working conditions, cargo influence) that affect corrosion processes are considered, it has been shown that corrosion will be initiated already after 7 years of use of the ship. In this case, it is most convenient to model the annual corrosion rate using a three-parameter Log-logistic distribution.

In this study, our primary focus has been on treating the parameter c_1 as a random variable within the probabilistic approach. This choice was informed by the significant influence of c_1 on the corrosion model

outcomes and the empirical data available for its estimation. By incorporating the variability of c_1, we aimed to capture the primary source of uncertainty in the corrosion process.

However, a fully probabilistic approach, which treats all parameters (c_1, c_2, and T_{cl}) as random variables, would provide a more comprehensive representation of uncertainties. Implementing such an approach would require extensive data to model the probability distributions of all parameters accurately, as well as sophisticated computational techniques to manage the increased complexity.

In future research, we plan to extend our probabilistic framework to incorporate random variables for c_2 and T_{cl} as well. This extension will enhance our uncertainty quantification, offering a more detailed understanding of the variability in the corrosion process and improving the robustness of our predictions.

Further research can be conducted on extended databases with more vessels, more thickness measurements and different input data on the operation and maintenance to consider sustainable structure. The analysis of more complex non-linear models of corrosive processes could be another direction of future research. This could provide more sophisticated tools for the design of reliable structural elements. Additionally, a cost-benefit analysis could be conducted using these models, to determine the optimal inspection and maintenance intervals that balance cost with the risk of corrosion damage.

ACKNOWLEDGEMENT

This research work has been supported by the INVAR-IVOŠEVIĆ Company. Some more information about the Company can be found at URL: http://www.invar.me/index.html. Namely, the data collected and systematised during the last twenty-five years by the Company operators and experts have been included into the above presented simulation and probabilistic analysis of the corrosion effects to the analysed group of ten aged bulk carriers` fuel tanks. It is to be pointed out that the INVAR-IVOŠEVIĆ Company provides its customers with marine services of ultrasonic thickness measurements of vessels' hull structures, and it has valid Certificates issued by recognised classification societies: LR, BV, DNV, RINA, KR and NKK. Currently, more than four hundred vessels (general cargo, bulk carriers, tankers, etc.) are being inspected by the Company.

REFERENCES

[1] United Nations, 2015. Transforming our World: The 2030 Agenda for Sustainable Development.

[2] International Maritime Organization, 2017. Linkages between IMO's Technical Assistance Work and the 2030 Agenda for Sustainable Development. London.

[3] International Maritime Organization, 2019. Strategy, planning and reform. London.

[4] International Maritime Organization, 2018. MEPC. Resolution MEPC.304(72) - Initial IMO strategy on reduction of GHG emissions from ships.: IMO, 2018/04/13.

[5] International Maritime Organization, 2020. MEPC. Resolution MEPC.324(75) - Amendments to the Annex of the Protocol of 1997 to amend the International Convention for the prevention of pollution from ships, 1973, as modified by the protocol of 1978 relating thereto. IMO, 2020/11/20.

[6] International Maritime Organization, 2018. MEPC. Resolution MEPC.308(73) - Guidelines on the Method of Calculation of the attained Energy Efficiency Design Index (EEDI) for new ships: IMO, 2018/10/26.

[7] International Maritime Organization, 2021. Draft report of the eight meeting of the Intersessional Working Group on Reduction of GHG Emissions from Ships (ISWG-GHG 8), 2021/05/28.

[8] Kalajdzic, M., Vasilev, M., Momcilovic, N., 2022. Assessment of Energy Efficiency for the Existing Cargo Ships, *Journal of Maritime Sciences*, 23(1), 33-46. https://doi.org/10.56080/jms220502

[9] Momcilovic, N., 2021. Countering the Climate Change Effects with Unconventional Design of Inland Vessels. *International Conference on Smart & Green Technology for Shipping and Maritime Industries – SMATECH 2021*, 21-22 October, Glasgow, UK.

[10] Knapp, S., Bijwaard, G., Heij, C., 2011. Estimated incident cost savings in shipping due to inspections. *Accident Analysis and Prevention*, 43, 1532–1539. https://doi.org/10.1016/j.aap.2011.03.005

[11] Heij, C., Knapp, S., 2019. Shipping inspections, detentions, and incidents: an empirical analysis of risk dimensions. *Maritime Policy & Management*, 46(7), 866–883. https://doi.org/10.1080/03088839.2019.1647362

[12] Poggi, L., Gaggero, T., Gaiotti, M., Ravina, E., Rizzo, C., 2020. Recent developments in remote inspections of ship structures. *International Journal of Naval Architect and Ocean Engineering*, 12, 881–891. https://doi.org/10.1016/j.ijnaoe.2020.09.001

[13] Ding, J.F., Tseng, W.J., Sung. Y.J., 2024. An evaluation of operational risks for general cargo ship operators. *Brodogradnja* 75(1), 75101. https://doi.org/10.21278/brod75101

[14] Barbulescu, A., Dumitriu, C.S., 2023. Fractal Characterization of Brass Corrosion in Cavitation Field in Seawater. *Sustainability*, 15, 3816. https://doi.org/10.3390/su15043816

[15] Brnic, J., Brcic, M., Balos, S., Vukelic, G., Krscanski, S., Milutinovic, M., Dramicanin, M., 2021. S235JRC+C Steel Response Analysis Subjected to Uniaxial Stress Tests in the Area of High Temperatures and Material Fatigue. *Sustainability*, 13, 5675. https://doi.org/10.3390/su13105675

[16] Paik, J.K., Thayamballi, A.K., Park, Y.I., 2003. Hwang, J.S. A time-dependent corrosion wastage model for bulk carrier structures. *International Journal of Marine Engineering*, 145(A2), 61–87. https://doi.org/10.3940/rina.ijme.2003.a2.18031

[17] Ivošević, Š., Meštrović, R., Kovač, N., 2017. An Approach to the Probabilistic Corrosion Rate Estimation Model for Inner Bottom Plates of Bulk Carrier. *Brodogradnja*, 68(4), 57-70. https://doi.org/10.21278/brod68404

[18] Perić, M., 2022. Prediction of cavitation on ships. *Brodogradnja*, 73(3), 39-58. https://doi.org/10.21278/brod73303

[19] Zriouel, W., Bentis, A., Majid, S., Hammouti, B., Gmouh, S., Umoren, P.S., Umoren, S.A., 2023. The Blue Tansy Essential Oil–Petra/Osiris/ Molinspiration (POM) Analyses and Prediction of Its Corrosion Inhibition Performance Based on Chemical Composition. *Sustainability*, 15, 14274. https://doi.org/10.3390/su151914274

[20] Wu, D., Hua, J., Chuang, S.-Y., Li, J., 2023. Preventative Biofouling Monitoring Technique for Sustainable Shipping. *Sustainability*, 15, 6260. https://doi.org/10.3390/su15076260

[21] Ramanavasu, R., Vijayakumar, K., Fernandez, S.G., 2023. Integrated Nanogrid for the Impressed Current Cathodic Protection System in Desalination Plant. *Sustainability*, 15, 7088. https://doi.org/10.3390/su15097088

[22] Rodkina, A., Ivanova, O., Kramar, V., Dushko, V., Zhilenkov, A., Chernyi, S., Zinchenko, A., 2022. Simulation and selection of a protection types in the design stage of ships and offshore structures. *Brodogradnja*, 73(2), 59-77.

[23] Ohyagi, M., 1987. Statistical Survey on Wear of Ships´ Structural Members. Nippon Kaiji Kyokai, *Technical Bulletin*, 5.

[24] Ivošević, Š., Kovač, N., Momčilović, N., Vukelić, G., 2021. Analysis of corrosion depth percentage on the inner bottom plates of aging bulk carriers with an aim to optimize corrosion margin. *Brodogradnja*, 72(3), 81-95. https://doi.org/10.21278/brod72306

[25] Yamamoto, N., Ikagaki, K.A., 1998. Study on the Degradation of Coating and Corrosion on Ship's Hull Based on the Probabilistic Approach. *Journal of Offshore Mechanics and Arctic Engineering*, 120, 121-128. https://doi.org/10.1115/1.2829532

[26] Nakai, T., Matsushita, H., Yamamoto, N., Arai, H., 2004. Effect of pitting corrosion on local strength of hold frames of bulk carriers (1st report). *Marine Structure*, 17, 403–432. https://doi.org/10.1016/j.marstruc.2004.10.001

[27] Garbatov, Y., Guedes Soares, C., 2008. Corrosion wastage modelling of deteriorated bulk carrier decks. *International Shipbuilding Progress*, 55, 109–125.

[28] Melchers, R. E., 2002. Effect of Temperature on the Marine Immersion Corrosion of Carbon Steels. *Corrosion*, 58(9), 768–782. https://doi.org/10.5006/1.3277660

[29] Soares, C.G., Garbatov, Y., 1999. Reliability of maintained, corrosion protected plates subjected to non–linear corrosion and compressive loads. *Marine Structure*, 12(6), 425–445. https://doi.org/10.1016/S0951-8339(99)00028-3

[30] Yamamoto, N., Kumano, A., Matoba, M., 1994. Effect of corrosion and its protection on hull strength (2nd Report). *Journal of the Society of Naval Architect of Japan*, 176, 281-289. https://doi.org/10.2534/jjasnaoe1968.1994.176_281

[31] Paik, J.K., Kim, S.K., Lee, S.K., 1998. A probabilistic corrosion rate estimation model for longitudinal strength members of bulk carriers. *Ocean Engineering*, 25(10), 837–860. https://doi.org/10.1016/S0029-8018(97)10009-9

[32] Paik, J.K., Lee, J.M., Park, Y.I., Hwang J.S., Kim, C.W., 2003. Time–variant ultimate longitudinal strength of corroded bulk carriers. *Marine Structure*, 16, 567–600. https://doi.org/10.1016/j.marstruc.2004.01.003

[33] Paik, J.K., Thayamballi, A.K., 2002. Ultimate strength of aging ships. *Journal of Engineering for the Marine Environmental*, 216(M1), 57–77. https://doi.org/10.1243/147509002320382149

[34] Paik, J.K., Wang, G., Thayamballi, A.K., Lee, J.M., Park, Y.I., Parunov, J., 2003. Time-dependent risk assessment of aging ships accounting for general/pit corrosion, fatigue cracking and local denting damage. *Transactions of the Society of Naval Architects and Marine Engineers*, 111, 159–197.

[35] Melchers, R.E., 1999. Corrosion uncertainty modelling for steel structures. *Journal of Constructional Steel Research*, 52(1 SU), 3–19. https://doi.org/10.1016/S0143-974X(99)00010-3

[36] Melchers, R.E., 2003. Probabilistic Model for Marine Corrosion of Steel for Structural Reliability Assessment. *Journal of Structural Engineering*, 129(11), 1484–1493. https://doi.org/10.1061/(ASCE)0733-9445(2003)129:11(1484)

[37] Melchers, R.E., 2006. Advances in Mathematical-Probabilistic Modelling of the Atmospheric Corrosion of Structural Steels in Ocean Environments, *3rd International ASRANet Colloquium*, 10-12 June, Glasgow, UK.

[38] Ivošević, Š., Meštrović, R., Kovač, N., 2019. Probabilistic estimates of corrosion rate of fuel tank structures of aging bulk carriers. *International Journal of Naval Architect and Ocean Engineering*, 11(1), 165-177. https://doi.org/10.1016/j.ijnaoe.2018.03.003

[39] Ivosevic, S., Mestrović, R., Kovac, N., 2020. A Probabilistic Method for Estimating the Percentage of Corrosion Depth on the Inner Bottom Plates of Aging Bulk Carriers. *Journal of Marine Science and Engineering*, 8(6), 442. https://doi.org/10.3390/jmse8060442

[40] Ivošević, Š., Kovač, N., Vastag, G. 2022. The analysis of the corrosion-induced failures of the inner bottom plating of fuel oil tanks. *15th International Symposium on Practical Design of Ships and Other Floating Structures* PRADS 2022, Dubrovnik, Croatia, 9-13 October, 457-467.

[41] Salmond, S., 2007. Taking the mystery out of research: Box and whisker plots: Displaying mean, interquartile range, and range. *Orthopaedic Nursing*, 26(1), 33. https://doi.org/10.1097/00006416-200701000-00010

[42] Qin, S., Cui, W., 2003. Effect of corrosion models on the time-dependent reliability of steel plated elements. *Marine Structures*, 16, 15-34. https://doi.org/10.1016/S0951-8339(02)00028-X

[43] Lovric, M., 2011. International encyclopedia of statistical science. *Springer*, Berlin, Heidelberg. https://doi.org/10.1007/978-3-642-04898-2

[44] Scheffe, H., 1999. The analysis of variance. *John Wiley & Sons*, 72.

[45] Devore, J. L., Berk, K. N., Carlton, M. A., 2021. Continuous random variables and probability distributions. In Modern Mathematical Statistics with Applications. *Cham: Springer International Publishing*. 189-275. ttps://doi.org/10.1007/978-3-030-55156-8_4

[46] Kovač, N., Ivošević, Š., Vastag, G., Vukelić, G., Rudolf, R., 2021. Statistical Approach to the Analysis of the Corrosive Behaviour of NiTi Alloys under the Influence of Different Seawater Environments. *Applied Sciences*, 11(19), 8825. https://doi.org/10.3390/app11198825

[47] Stephens, M. A., 1992. Introduction to Kolmogorov (1933) on the empirical determination of a distribution. In Breakthroughs in Statistics: Methodology and Distribution. *Springer*, New York, 93-105. https://doi.org/10.1007/978-1-4612-4380-9_9